Comparison of Branched-Chain and Tightly Coupled Reaction Mechanisms for Prostaglandin H Synthase†

Chunhong Wei, Richard J. Kulmacz, and Ah-Lim Tsai*

Division of Hematology, Department of Internal Medicine, University of Texas Health Science Center at Houston, Houston, Texas 77030

Received January 11, 1995; Revised Manuscript Received April 7, 1995⊗

ABSTRACT: Two types of mechanisms have been proposed to account for the combination of peroxidase and cyclooxygenase activities in prostaglandin H synthase (PGHS). One, a branched-chain mechanism [Dietz, R., et al. (1988) *Eur. J. Biochem. 171*, 321−328], postulates that the cyclooxygenase reaction propagates essentially independently of peroxidase catalysis. The second, a tightly coupled mechanism [Bakovic, M., & Dunford, H. B. (1994) *Biochemistry 33*, 6475−6482], postulates that peroxidase catalysis is an integral part of cyclooxygenase propagation. Qualitative and quantitative predictions from the two mechanisms have been compared with several observed characteristics of the PGHS reaction with arachidonate, including the ability to accumulate PGG_2 and oxidized enzyme intermediates, the stoichiometry between cosubstrate and fatty acid consumption, and the hydroperoxide activator requirement. The observed characteristics, particularly the accumulation of micromolar levels of PGG_2 even in the presence of cosubstrate and the stoichiometry between cosubstrate oxidation and fatty acid oxygenation of less than 1.3 (compared to a theoretical maximum of 2.0), were largely consistent with predictions from the branched-chain mechanism, but contradicted important predictions of the tightly coupled mechanism. These results indicate that PGHS catalysis is more accurately described by the branched-chain mechanism than by the tightly coupled mechanism.

Prostaglandin H synthase (PGHS)[1] has two distinct catalytic activities: a cyclooxygenase activity, which converts arachidonate to PGG_2, and a peroxidase activity, which converts PGG_2 to PGH_2 (van der Ouderaa et al., 1977). Initiation of the cyclooxygenase activity is known to require hydroperoxides (Smith & Lands, 1972), and considerable evidence indicates that cyclooxygenase initiation involves transient generation of oxidized peroxidase catalytic intermediates (Smith et al., 1992). The mechanism for coupling of the PGHS cyclooxygenase and peroxidase catalytic cycles has been controversial. One proposal (Dietz et al., 1988) suggests that peroxidase compound I [Fe(IV)PP•] is the precursor of the first cyclooxygenase cycle intermediate, but that otherwise the peroxidase and cyclooxygenase cycles operate independently, as depicted in Scheme 1. In this mechanism, PGG_2 produced by one PGHS molecule initiates cyclooxygenase catalysis in many other PGHS molecules. The concentration of PGHS involved in cyclooxygenase propagation thus increases as the reaction progresses, a hallmark of autocatalytic or branched-chain reactions (Boudart, 1968). A second proposal (Bakovic & Dunford, 1994) suggests that the peroxidase and cyclooxygenase cycles are fused, with peroxidase compound I serving as the primary oxidant in cyclooxygenase catalysis, as depicted in Scheme 2. The shared enzyme intermediate in this mechanism results in tight coupling between the cyclooxygenase and peroxidase catalytic cycles.

Scheme 1: Hypothetical Branched-Chain Mechanism Based on That Proposed by Dietz et al. (1988)[a]

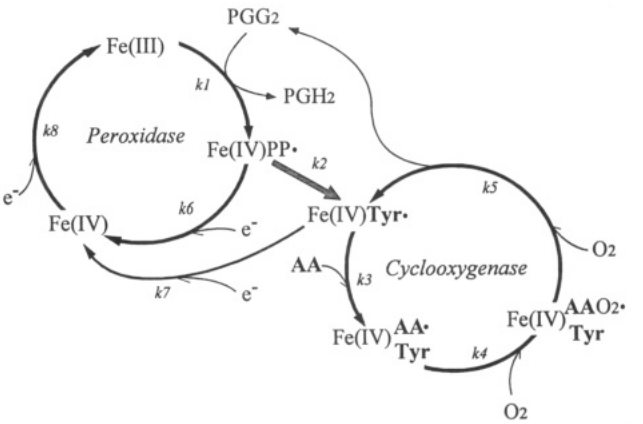

[a] Roman numerals indicate the oxidation state of the heme iron. Fe(III), resting enzyme; Fe(IV)PP•, compound I; e^-, reducing equivalent furnished by ferulate or other cosubstrate; Fe(IV), compound II; Fe(IV)Tyr•, enzyme with tyrosyl radical; Fe(IV)AA•/Tyr, enzyme with bound fatty acid radical; Fe(IV)AAO_2•/Tyr, enzyme with bound fatty acid hydroperoxy radical.

One striking difference between the two mechanisms is in their predictions of the ability to accumulate PGG_2 during reaction with arachidonate. In the branched-chain mechanism (Scheme 1), initial reaction of PGHS with hydroperoxide is required to initiate cyclooxygenase activity, but subsequent cyclooxygenase catalysis proceeds independently of peroxidase cycle reactions. The rate of PGG_2 synthesis

† This work was supported in part by NIH Grant GM 44911.

* Author to whom correspondence should be addressed at the Division of Hematology, Department of Internal Medicine, University of Texas Health Science Center, 6431 Fannin St., Houston, TX 77030; telephone 713-792-5450, fax 713-794-4230.

⊗ Abstract published in *Advance ACS Abstracts,* June 1, 1995.

[1] Abbreviations: PGHS, prostaglandin H synthase; PG, prostaglandin; AA, arachidonic acid; FA, ferulic acid; 15-HPETE, 15-hydroperoxyeicosa-5,8,11,13-tetraenoic acid; 15-HETE, 15-hydroxyeicosa-5,8,-11,13-tetraenoic acid; TMPD, *N,N,N′,N′*-tetramethyl-*p*-phenylenediamine.

0006-2960/95/0434-8499$09.00/0

Scheme 2: Hypothetical Tightly Coupled Mechanism Based on That Proposed by Bakovic and Dunford (1994)[a]

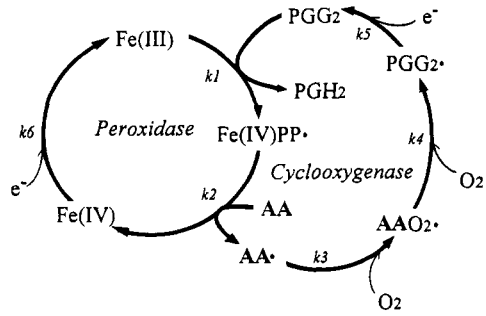

[a] Roman numerals indicate the oxidation state of the heme iron: Fe(III), resting enzyme; Fe(IV)PP•, compound I; e^-, reducing equivalent furnished by ferulate or other cosubstrate; Fe(IV), compound II; AAO_2•, fatty acid hydroperoxy radical; PGG_2•, PGG_2 hydroperoxy radical.

by the cyclooxygenase thus is not coupled to the rate of PGG_2 reduction by the peroxidase, except at the very beginning of the reaction. As a consequence, the form of the branched-chain mechanism permits transient PGG_2 accumulation during reaction of PGHS with arachidonate. In contrast, in the tightly coupled mechanism (Scheme 2) the active cyclooxygenase intermediate, Fe(IV)PP•, is returned to the resting state at the end of each cycle and must be reactivated by reaction with another mole of PGG_2. Each cycle of the reaction results in the consumption and synthesis of equal amounts of PGG_2. Thus, the tightly coupled mechanism predicts that PGG_2 cannot accumulate beyond the level of hydroperoxide initially present. As a consequence of these differences, accumulation of PGG_2 during reaction of PGHS with arachidonate provides one clear test of the branched and tightly coupled types of reaction mechanisms shown in Schemes 1 and 2. Published evidence on the point is ambivalent. Some workers reported finding PGG_2 or its degradation product during the reaction (Kulmacz, 1987; Eling et al., 1991), whereas others found mostly PGH_2, especially when higher levels of peroxidase cosubstrate were present (Egan et al., 1976; Graff, 1982). To resolve this issue, we have performed a kinetic analysis of arachidonate metabolites during reaction of PGHS with arachidonate and cosubstrate under a variety of conditions.

A second major difference between the two mechanisms is in the expected stoichiometry between peroxidase and cyclooxygenase catalysis. With the tightly coupled mechanism, the peroxidase and cyclooxygenase cycles are locked together (Scheme 2), so that exactly 2 equiv of reducing cosubstrate are consumed for each mole of arachidonate oxygenated. In contrast, the branched-chain mechanism (Scheme 1) permits cyclooxygenase propagation without continued peroxidase catalysis and, thus, allows any stoichiometry less than 2 equiv of cosubstrate/mol of fatty acid. Bakovic and Dunford (1994) reported a stoichiometry of roughly 2, which was taken to support the tightly coupled mechanism. However, Bakovic and Dunford (1994) did not correct the cyclooxygenase velocities for the considerable damping effect that the oxygen electrode membrane has on electrode responsiveness (Cook et al., 1979). The lack of such correction leads to substantial underestimation of the true cyclooxygenase velocity and overestimation of the peroxidase/cyclooxygenase stoichiometry. Because of this uncertainty and the usefulness of the stoichiometry in assessing the degree of coupling between the two activities in PGHS, we have reevaluated the peroxidase/cyclooxygenase ratio for reactions with many combinations of cosubstrate and fatty acid levels.

For additional tests, we have compared other experimental observations with the corresponding reaction characteristics predicted by the branched-chain and tightly coupled mechanisms. Overall, the present examination of many aspects of the PGHS reaction with arachidonate provides strong support for the branched-chain mechanism and argues against the tightly coupled mechanism.

MATERIALS AND METHODS

Hemin chloride, TMPD, and ferulic acid were obtained from Sigma Chemical Co. (St. Louis, MO). Ferulic acid was recrystallized from water before use. Arachidonic acid was purchased from NuChek Preps, Inc. (Elysian, MN), and treated with sodium borohydride to decompose hydroperoxides (Kulmacz & Lands, 1987). [1-^{14}C]Arachidonic acid was from Amersham Corporation (Arlington, IL) and used without further treatment. Prostaglandin standards were purchased from Cayman Chemical (Ann Arbor, MI).

PGHS was purified to homogeneity from sheep seminal vesicles and reconstituted with hemin; quantitation of the holoenzyme concentration was based on the heme concentration determined from the Soret absorbance (Kulmacz et al., 1987). The same batch of enzyme was used for both cyclooxygenase and peroxidase reactions to facilitate direct comparison. Cyclooxygenase activity was monitored with a Yellow Springs Instrument Co. (Yellow Springs, OH) Model 53 oxygen meter (Kulmacz & Lands, 1987). The oxygen electrode was covered with a standard Teflon membrane supplied by the manufacturer. The signal from the oxygen meter was digitized with a Remote Measurement Systems (Seattle, WA) Model ADC-1 A/D converter connected to a Macintosh SE computer. Reactions at 25 °C were started by the addition of enzyme (generally 35 nM heme) to a cuvette containing 3 mL of 0.1 M potassium phosphate (pH 8.0) and various levels of arachidonate and reducing cosubstrate. The Teflon membrane covering the polarographic electrode has a finite permeability to oxygen (Cook et al., 1979). Because of this impeded oxygen transport, the electrode response lags changes in oxygen concentration during the cyclooxygenase reaction. The formula used to correct for the membrane effect is

$$[O_2]_c(t) = [O_2]_e(t) + \{[O_2]_e(t+1) - [O_2]_e(t)\}/\{k\Delta t\} \quad (1)$$

where $[O_2]_c(t)$ is the O_2 concentration in the cuvette (outside the membrane) at time t, $[O_2]_e(t)$ and $[O_2]_e(t+1)$ are the O_2 concentrations detected by the electrode (inside the membrane) at time points t and $t+1$, k is an empirical diffusion rate constant, and Δt is the time interval between data points. The value of k is determined from the exponential relaxation kinetics of the electrode signal after injection of nitrogen-saturated buffer into a reaction cuvette previously equilibrated with air (Cook et al., 1979). A value of 0.22 s^{-1} was calculated for k at 25 °C in the present study. This is in good agreement with the value of 0.24 s^{-1} found for k at 30 °C (Cook et al., 1979).

PGG_2 and PGH_2 levels during reactions of PGHS with arachidonate were quantitated by using radiolabeled fatty acid. The incubation mixtures contained 0.3 mL of 0.1 M potassium phosphate (pH 8.0), the desired concentration of

cosubstrate, and holoenzyme (35 nM) in continuously stirred glass tubes maintained at 25 °C. Reactions were initiated by the addition of 20−80 μM [^{14}C]arachidonate (9 mCi/mmol) in a small volume of ethanol (final concentration <1%), and they were quenched after 2−400 s by the addition of 3 vol of ice-cold diethyl ether/methanol/2 M citric acid (30:4:0.5) and vigorous mixing. For zero point controls, the quench solvent was added before the arachidonate. The lipid extracts were dried by addition of anhydrous Na_2SO_4 and reduced to a small volume by evaporation under a stream of nitrogen gas. Aliquots of the concentrated extracts were then separated by thin-layer chromatography at 0 °C on Whatman LK6D silica gel plates, using 50 μg of unlabeled arachidonic acid as the carrier in each lane and diethyl ether/hexane/acetic acid (85:15:0.1) as the developing solvent. Metabolite bands were visualized by autoradiography, and their positions on the plate were marked with a needle while the film was superimposed on the silica layer. Individual fractions from the entire length of each lane were scraped into vials, and their radioactivity was determined by liquid scintillation counting. The concentration of each metabolite was calculated by multiplying the fraction of total radioactivity in that metabolite band, corrected for the corresponding band in the zero time control, by the initial arachidonate concentration.

Peroxidase activity was monitored at 25 °C in a stirred cuvette with a Shimadzu Model 2101PC UV−vis scanning spectrophotometer. The reaction mixture contained 2 mL of 0.1 M potassium phosphate (pH 8.0), PGHS holoenzyme (35 nM), and various levels of arachidonate and reducing cosubstrate. Ferulic acid oxidation was followed by absorbance changes at 310 nm using a difference absorption coefficient of 7.34 mM^{-1} cm^{-1} (Bakovic & Dunford, 1994).

Self-inactivation of the peroxidase activity was also followed spectrophotometrically. For this, the enzyme (35 nM) was reacted with excess arachidonate (80 μM) and ferulate (100 μM). The surviving peroxidase capacity at later times in the reaction was determined from the absorbance change at 310 nm caused by the addition of 20 μM 15-HPETE.

Computer simulations of detailed reaction kinetics predicted by the individual reaction mechanisms were done by numerical integration of the combined rate equations, using the SCoP program (Simulation Resources Inc., Berrien Springs, MI). The mechanisms are shown in Schemes 1 and 2; the individual rate equations and the values of the rate constants used are listed in Tables 1 and 2.

Branched-Chain Mechanism (Scheme 1). The formulation is based on the mechanism proposed by Dietz et al. (1988). The individual reaction steps and the values of the rate constants used in the simulations are shown in Table 1. The values of k_1 and k_2 are based on reported values (Dietz et al., 1988) and measurements of the temperature dependence of these rates.[2] The observed isotope effect (Hamberg & Samuelsson, 1967) makes it likely that k_3 is the rate-limiting step of the cyclooxygenase cycle. Experimental estimates for the value of k_3 can be obtained in two ways. The first method is based on the specific activity of the batch of PGHS used here: 70 units/μg protein in the standard assay at 30 °C with a saturating level of arachidonate (100 μM). After correction for the electrode membrane effect and the temperature difference, this is equivalent to a turnover number of 80 s^{-1} at 25 °C and a k_3 value of 8 × 10^5 M^{-1} s^{-1}. The value of k_3 also can be estimated from the number of cyclooxygenase turnovers before self-inactivation and the rate of cyclooxygenase self-inactivation. For this calculation, self-inactivation is assumed to occur exclusively by an abortive side reaction of the tyrosyl radical species [Fe(IV)-Tyr$^\bullet$ → E_{dead}], governed by rate constant k_9. The number of turnovers before self-inactivation is then determined by the ratio of the rates for two of the reactions involving Fe(IV)Tyr$^\bullet$: cyclooxygenase catalysis via the k_3 process and inactivation via the k_9 process. The k_7 step is irrelevant in this context because it does not affect the number of cyclooxygenase turnovers before self-inactivation. Thus,

$$\#\ \text{cyclooxygenase turnovers} = k_3[\text{arachidonate}]/k_9 \quad (2)$$

and

$$k_3 = \#\ \text{cyclooxygenase turnovers}\ (k_9)/[\text{arachidonate}] \quad (3)$$

For reaction with 80 μM arachidonate and 100 μM ferulate, the cyclooxygenase was found to turn over 200 times before self-inactivation (Results), and the cyclooxygenase velocity was found to decay at 0.42 s^{-1}. This leads to a value of 1.0 × 10^6 M^{-1} s^{-1} for k_3, which is in good agreement with the value calculated from the specific activity.

Table 1: Reaction Steps and Rate Constants for the Branched-Chain Mechanism Shown in Scheme 1

reaction step	rate constant	value[a]
Fe(III) + PGG_2 → Fe(IV)PP$^\bullet$ + PGH_2	k_1	1 × 10^8 M^{-1} s^{-1}
Fe(IV)PP$^\bullet$ → Fe(IV)Tyr$^\bullet$	k_2	350 s^{-1}
Fe(IV)Tyr$^\bullet$ + AA → Fe(IV)AA$^\bullet$/Tyr	k_3	1 × 10^6 M^{-1} s^{-1}
Fe(IV)AA$^\bullet$/Tyr + O_2 → Fe(IV)$AAO_2^\bullet$/Tyr	k_4	≥5 × 10^6 M^{-1} s^{-1}
Fe(IV)$AAO_2^\bullet$/Tyr + O_2 → Fe(IV)Tyr$^\bullet$ + PGG_2	k_5	≥5 × 10^6 M^{-1} s^{-1}
Fe(IV)PP$^\bullet$ + FA[b] → Fe(IV) + FA$^\bullet$	k_6	≤3.5 × 10^6 M^{-1} s^{-1}
Fe(IV)Tyr$^\bullet$ + FA[b] → Fe(IV) + FA$^\bullet$	k_7	(0.5−5) × 10^6 M^{-1} s^{-1}
Fe(IV) + FA[b] → Fe(III) + FA$^\bullet$	k_8	5.5 × 10^6 M^{-1} s^{-1}

[a] The values for k_1, k_2, k_3, and k_8 were based on experimental measurements; the other values indicate the ranges found to predict a cyclooxygenase velocity within 30% of that observed. Details are described in Materials and Methods. [b] For simplicity, only the electron (e^-) donated by ferulic acid is shown in Scheme 1.

Table 2: Reaction Steps and Rate Constants for the Tightly Coupled Mechanism Shown in Scheme 2

reaction step	rate constant	value[a]
Fe(III) + PGG_2 → Fe(IV)PP$^\bullet$ + PGH_2	k_1	1 × 10^8 M^{-1} s^{-1}
Fe(IV)PP$^\bullet$ + AA → Fe(IV) + AA$^\bullet$	k_2	1 × 10^6 M^{-1} s^{-1}
AA$^\bullet$ + O_2 → $AAO_2^\bullet$	k_3	≥5 × 10^5 M^{-1} s^{-1}
$AAO_2^\bullet$ + O_2 → $PGG_2^\bullet$	k_4	≥5 × 10^5 M^{-1} s^{-1}
$PGG_2^\bullet$ + FA[b] → PGG_2 + FA$^\bullet$	k_5	≥5 × 10^5 M^{-1} s^{-1}
Fe(IV) + FA[b] → Fe(III) + FA$^\bullet$	k_6	5.5 × 10^6 M^{-1} s^{-1}

[a] The values for k_1 and k_6 were based on experimental measurements, k_2 was assigned the same value as that for the similar step in the branched-chain mechanism (k_3 in Scheme 1), and the other values are those that decreased the predicted cyclooxygenase velocity by less than 30% from the maximal velocity. Details are described in Materials and Methods. [b] For simplicity, only the electron (e^-) donated by ferulic acid is shown in Scheme 2.

[2] A.-L. Tsai, C. Wei, H. K. Baek, R. J. Kulmacz, and H. E. Van Wart, unpublished results.

Table 3: Effect of Rate Constant Values on Peak Cyclooxygenase Velocity Predicted by the Tightly Coupled Mechanism[a]

k_5 (M^{-1} s^{-1})	k_2 (M^{-1} s^{-1})				
	10^5	10^6	10^7	10^8	10^9
	Peak Oxygenase Rate ($\mu M s^{-1}$)				
10^5	0.07	0.10	0.10	0.10	0.10
10^6	0.08	0.13	0.13	0.13	0.13
10^7	0.09	0.13	0.14	0.14	0.14
10^8	0.09	0.13	0.14	0.14	0.14
10^9	0.09	0.13	0.14	0.14	0.14

[a] Reactions for 35 nM PGHS, 80 μM arachidonate, 100 μM ferulate, and an initial hydroperoxide level of 20 nM were simulated with the indicated values for k_2 and k_5 and the other parameter values as shown in Table 2.

With k_3 taken to be rate determining for cyclooxygenase catalysis, the values of k_4 and k_5 are simply set larger than that of k_3. The k_4 and k_5 steps are included simply to reflect likely stages in the chemical transformation of substrate; the precise values for k_4 and k_5 have no effect on the simulation, as long as they are significantly larger than k_3.

The value of the rate constant for reaction of compound II [Fe(IV) in Scheme 1] with ferulic acid (k_8) is that reported by Bakovic and Dunford (1994). It is worth noting that the mechanism in Scheme 1 has two peroxidase catalytic pathways: one via the k_1, k_6, and k_8 steps and the other via the k_1, k_2, k_7, and k_8 steps. The kinetics of tyrosyl radical EPR intensity has been found to correlate reasonably well with optical changes at 560 nm ascribed to ferryl heme intermediates (Tsai et al., 1992), suggesting that the tyrosyl radical species [Fe(IV)Tyr$^\bullet$ in Scheme 1] can be a major ferryl species. In line with this, the relative values of k_2 and k_6 are such that much of peroxidase catalysis in the simulation occurs via the k_2 step, except at very high cosubstrate levels. An upper limit for k_6 of 3.5×10^6 M^{-1} s^{-1} was thus estimated from the value of k_2. In fact, our simulations showed that k_6 could be varied up to 4 orders below this upper limit without appreciably changing the overall oxygen consumption rate. Little is known about the value of k_7. We ran simulations with several combinations of values for k_3 and k_7, varying k_3 over $(0.2-5) \times 10^6$ M^{-1} s^{-1} and k_7 over $(0.05-5) \times 10^6$ M^{-1} s^{-1}, and found that reasonable cyclooxygenase velocities (within 30% of the observed rate) were predicted from a fairly wide range of combinations of k_3 and k_7.

Tightly Coupled Mechanism (Scheme 2). The formulation is that proposed by Bakovic and Dunford (1994). The individual reaction steps and the rate constants used in the simulations are shown in Table 2. The values of k_1 and k_6 are the same as those of k_1 and k_8 in the branched-chain mechanism (Scheme 1). Reaction of compound I with ferulate was not explicitly included in the original formulation of the tightly coupled mechanism (Bakovic & Dunford, 1994), and so it was not included in the present simulations. As with the branched-chain mechanism, steps involving reactions of organic radicals with O_2 are likely to be very fast, so values close to the diffusion limit were used for k_3 or k_4; the precise values of these rate constants do not affect the kinetic simulations. This leaves either k_2 or k_5 as the potential rate-limiting step for the cycle. The effect of these parameters on the predicted cyclooxygenase kinetics was examined by simulating reactions with combinations of k_2 and k_5 values ranging from 10^5 to 10^9 M^{-1} s^{-1} (Table 3).

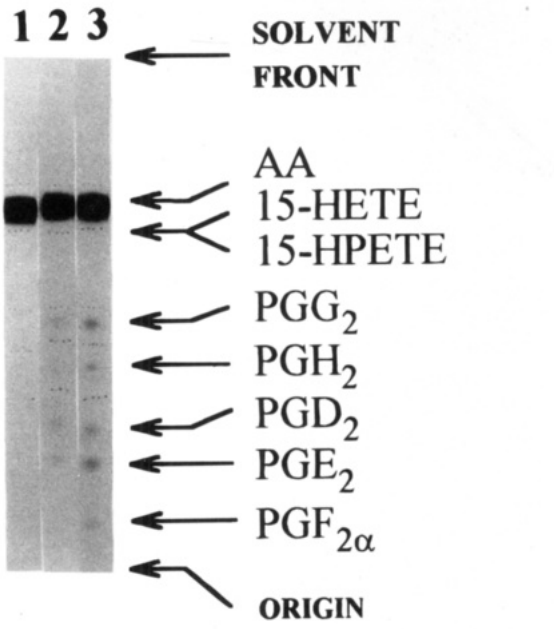

FIGURE 1: Thin-layer chromatography of [^{14}C]arachidonic acid metabolites from reaction with PGHS in 0.1 M phosphate buffer (pH 8.0) at 25 °C: lane 1, 80 μM AA/100 μM FA/35 nM PGHS, zero time control; lane 2, 80 μM AA/no FA/35 nM PGHS, at 20 s; lane 3, 80 μM AA/100 μM FA/35 nM PGHS, at 20 s. Mobilities of standards are shown by arrows. The dots are needle marks used to locate bands for scintillation counting.

The predicted peak oxygen consumption rate varied by only a factor of 2 over the entire range of k_2 and k_5 values tested, indicating that the choice of these values was not crucial to the reaction kinetics predicted by the tightly coupled mechanism. For the remaining simulations, k_2 was set at 1×10^6 M^{-1} s^{-1} and k_5 was set at 1×10^8 M^{-1} s^{-1}.

RESULTS

Kinetics of PGG_2 and PGH_2 Formation during Reaction of PGHS with [^{14}C] Arachidonic Acid. Reaction of PGHS with [^{14}C]arachidonate in the absence of cosubstrate produced several polar metabolites (Figure 1). The major metabolite, with an R_f value of 0.48, comigrated with standard PGG_2, and a more polar metabolite, with an R_f value of 0.40, comigrated with standard PGH_2. These two bands also comigrated with the same standards when the plate was developed with a different solvent [the A9 solvent system in Hurst et al. (1987); data not shown], supporting the identification of these metabolites as PGG_2 and PGH_2. Smaller amounts of metabolites with R_f values of 0.28, 0.22, and 0.12 were also observed. When ferulic acid or phenol was included in the reaction mixture, more of the arachidonate was oxygenated, with a larger increase in PGH_2 than in PGG_2 (Figure 1). These changes are expected, given the ability of ferulate and phenol to stimulate cyclooxygenase activity and to act as a peroxidase cosubstrate in the conversion of PGG_2 to PGH_2 (Egan et al., 1976; Bakovic & Dunford, 1994). The presence of additional products besides PGG_2 and PGH_2 is also expected because these compounds are labile in water, and because the cyclooxygenase is known to produce a number of side products (Hecker et al., 1987).

A detailed analysis of the PGG_2 and PGH_2 concentrations during reactions of PGHS with [^{14}C]arachidonate, with and without reducing cosubstrates, is presented in Figure 2. In the absence of cosubstrate (panel A), the levels of PGG_2 were

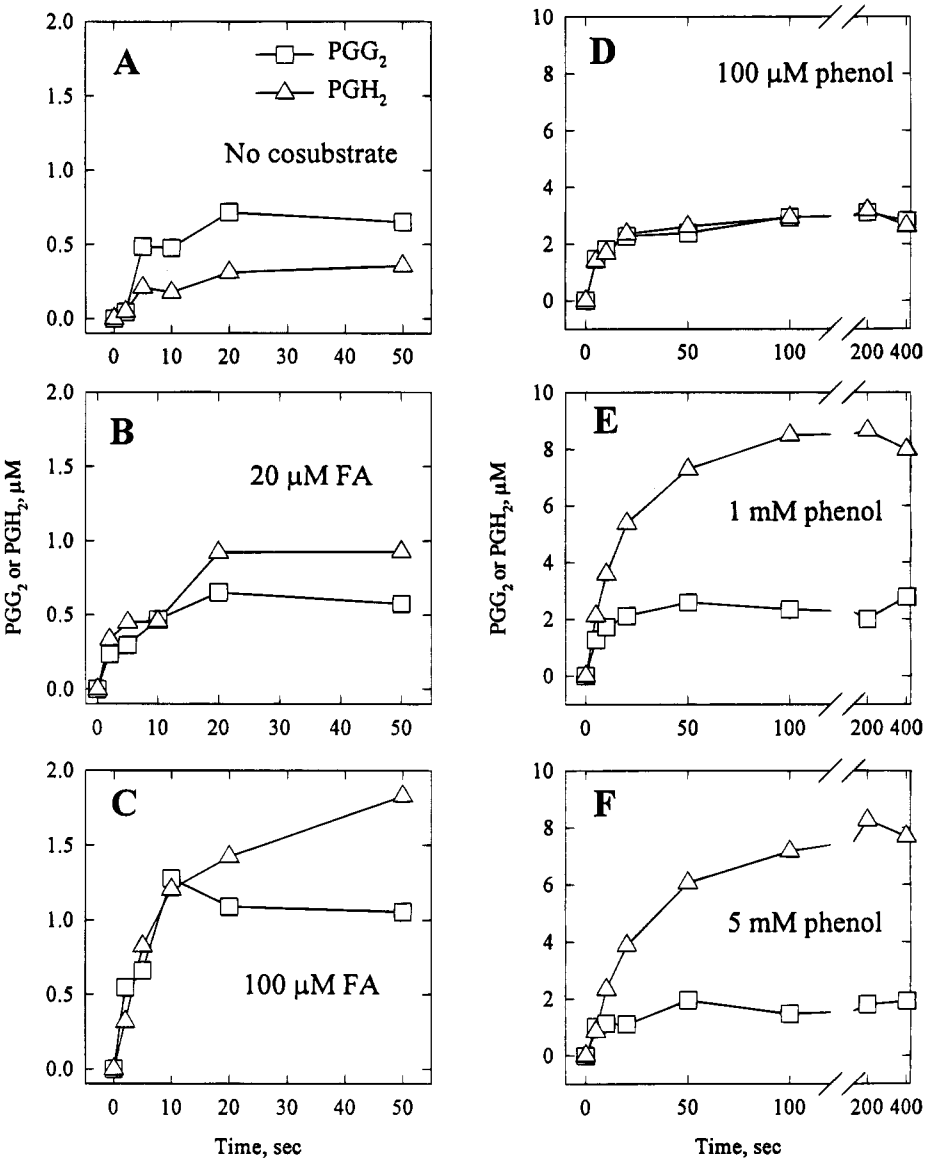

FIGURE 2: Kinetics of PGG_2 and PGH_2 accumulation during reaction of PGHS with arachidonate. The concentrations of PGG_2 (□) and PGH_2 (△) were determined at various times after the addition of 80 μM [^{14}C]arachidonate to reaction mixtures containing 35 nM PGHS and the indicated levels of either ferulate or phenol.

about twice those of PGH_2 throughout the reaction. Maximal levels (0.7 μM PGG_2 and 0.3 μM PGH_2) were reached at about 20 s and did not decline much afterward. The total concentration of arachidonate metabolites at 50 s was 1.9 μM, representing 55 cyclooxygenase catalytic cycles before self-inactivation. Inclusion of a low level of ferulic acid (20 μM) in the reaction did not much alter the kinetics of PGG_2 production, but it did increase the PGH_2 levels markedly, so that they exceeded those of PGG_2 (Figure 2, panel B). The arachidonate metabolite concentration at 50 s was 3.5 μM, or about 100 catalytic cycles before self-inactivation. With a higher level of ferulate present (100 μM), the levels of both PGG_2 and PGH_2 were increased further, again with PGH_2 in excess of PGG_2 at the later points (Figure 2, panel C). With 100 μM ferulate, the sum of arachidonate metabolite concentrations at 50 s was 6.9 μM, or about 200 catalytic cycles before self-inactivation. Cyclooxygenase activity measured with the oxygen electrode was increased by 15% with 20 μM ferulate and by 61% with 100 μM ferulate compared to the control reaction.

Arachidonate metabolite kinetics was also examined with phenol as the cosubstrate. The metabolites produced in the presence of phenol had the same chromatographic mobilities as those shown in Figure 1 for metabolites formed in the presence of ferulic acid (data not shown). With 100 μM phenol, the kinetics of PGG_2 accumulation was almost superimposable on that of PGH_2, with both rising rapidly in the first 20 s and then more slowly later, with both reaching peak levels of about 3 μM after 200 s (Figure 2, Panel D). With 100 μM phenol, the sum of arachidonate metabolite concentrations at 200 s was 7.7 μM, or about 220 catalytic cycles before self-inactivation. With 1 mM phenol there was little change in PGG_2 kinetics, but the accumulation of PGH_2 was more gradual and sustained, reaching a peak of 8.5 μM at 200 s; this PGH_2 level was over 4 times that of PGG_2 (Figure 2, panel E). With 1 mM phenol, the sum of arachidonate metabolite concentrations at 200 s was 13.8 μM, or about 390 catalytic cycles before self-inactivation. When the phenol level was increased to 5 mM the rates of PGG_2 and PGH_2 accumulation were much slower than those at 1

mM phenol, and the peak levels at 200 s were somewhat lower (Figure 2, panel F). With 5 mM phenol, the sum of arachidonate metabolite concentrations at 200 s was 13.1 μM, or about 370 catalytic cycles before self-inactivation. The cyclooxygenase activity measured with the oxygen electrode was increased by 83% with 100 μM phenol, by 91% with 1 mM phenol, and by only 1% with 5 mM phenol. The consistent result in the data in Figure 2 is that PGG_2 accumulated to significant level under all conditions examined, even in the presence of enough cosubstrate to maximally stimulate the cyclooxygenase velocity. Regardless of the precise peak concentrations, the reproducible observation of PGG_2 accumulation is inconsistent with the tightly coupled mechanism, which requires that exactly 1 mol of PGG_2 be reduced and exactly 1 mol of arachidonate be oxygenated in each catalytic cycle (Scheme 2), keeping the PGG_2 concentration at its initial level. The branched-chain mechanism, in contrast, requires PGG_2 reduction only for cyclooxygenase initiation and not for cyclooxygenase propagation (Scheme 1) and, thus, permits the accumulation of PGG_2.

Comparison of Rates of Ferulate Oxidation and Arachidonate Oxygenation. The ratio between peroxidase and cyclooxygenase velocities has been used as the primary criterion to distinguish between the tightly coupled and branched-chain mechanisms for PGHS (Bakovic & Dunford, 1994). Accordingly, the cyclooxygenase and peroxidase velocities were continuously monitored in reactions with a variety of ferulate and arachidonate concentrations. The results with 80 μM arachidonate and 100 μM ferulate are shown as examples in Figure 3. The peroxidase velocity declined quickly from its maximal value (2.4 μM ferulate s^{-1}) and approached zero by 20 s (Figure 3, top). The corresponding cyclooxygenase velocity, before correction for the membrane effect, displayed a significant lag, reaching a maximum of 1.4 μM O_2 s^{-1} only after 4 s (Figure 3, middle). No lag was seen in the peroxidase reaction kinetics (Figure 3, top). However, the apparent cyclooxygenase lag disappeared and the velocity was considerably higher (2.9 μM O_2 s^{-1} in this reaction) once correction was made for the damping effect of the electrode membrane, as described in Materials and Methods (Figure 3, bottom).

When the corrected peak cyclooxygenase velocities were plotted as a function of the corresponding peak electrode signal velocities, the points appeared to fall on a straight line (inset to Figure 3, bottom). The slope of this line determined by linear regression was 1.81, the *y*-intercept was 0.42 μM O_2 s^{-1}, and the *r* value was 0.93. This indicates that the damping effect of the electrode membrane led to underestimation of the actual oxygen consumption rate by almost a factor of 2. The data set for the Figure 3 inset includes reactions with a wide range of ferulate, phenol, and arachidonate concentrations. Subsets of the data, from reactions with either ferulate, phenol, TMPD, or no cosubstrate, were each distributed evenly along the same fitted line (not shown). This indicates that the relationship between the corrected and observed velocities was insensitive to cosubstrate concentration and identity. The linear relationship found in the Figure 3 inset data thus provides a reliable and convenient way to calculate the corrected peak oxygen consumption velocities from the corresponding peak electrode velocities.

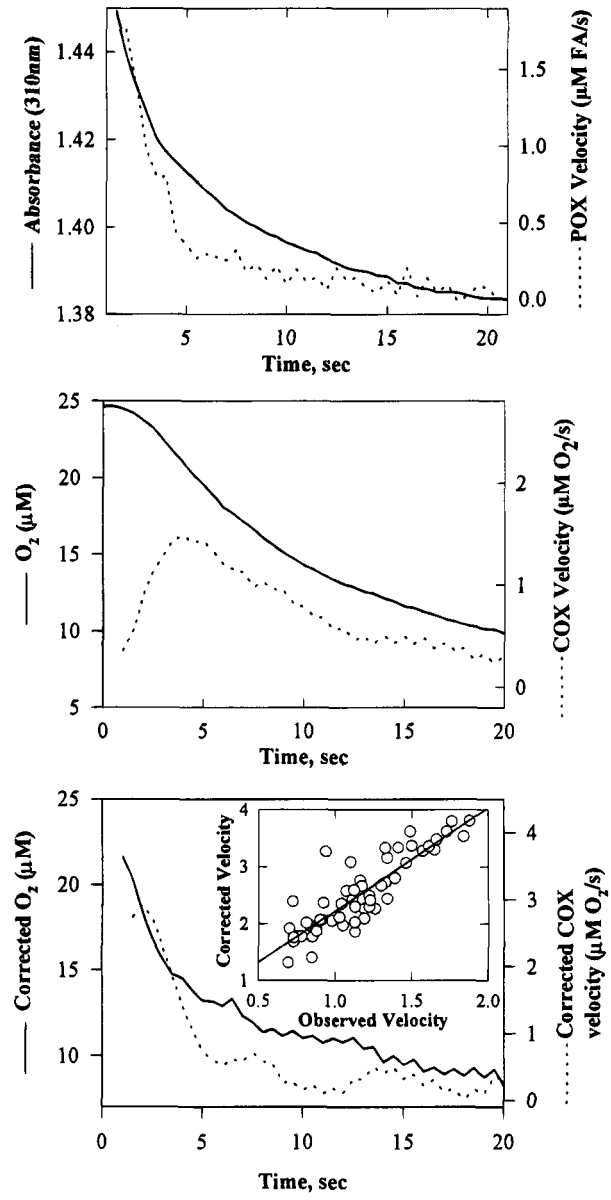

FIGURE 3: Oxygenase and peroxidase kinetics during reaction of PGHS with arachidonate. PGHS holoenzyme (35 nM) in 0.1 M potassium phosphate (pH 8.0) at 25 °C was reacted with 80 μM AA and 100 μM FA. Peroxidase and cyclooxygenase kinetics were monitored as described in Materials and Methods. Upper panel: Absorbance changes at 310 nm (—) and the peroxidase velocity values calculated from the ferulate oxidation (- - -) at 0.5 s intervals. Middle panel: Uncorrected oxygen concentrations (—) and the corresponding cyclooxygenase velocities (- - -) at 0.5 s intervals. Lower panel: Oxygen concentrations corrected for the electrode membrane damping by using eq 1 (—) and the corresponding corrected cyclooxygenase velocities (- - -) at 0.5 s intervals. Lower panel inset: The maximal oxygenase velocities calculated from corrected oxygen consumption data are plotted as a function of the maximal oxygenase velocities calculated from the raw oxygen electrode data for reactions of PGHS (35 nM) in 0.1 M potassium phosphate (pH 8.0) at 25 °C with 20–80 μM arachidonate in the presence of 0–100 μM ferulate, 0–500 μM phenol, or 0–84 μM TMPD. The line represents the linear regression (r = 0.93).

The ratios of the peak peroxidase and corrected cyclooxygenase rates for a series of reactions with 20, 40, or 80 μM arachidonate and 0, 20, 50, or 100 μM ferulate are plotted as a function of the ratio of initial ferulate to arachidonate levels in Figure 4. There was considerable variation in the value of the rates ratio, which ranged from 0.39 to 0.89

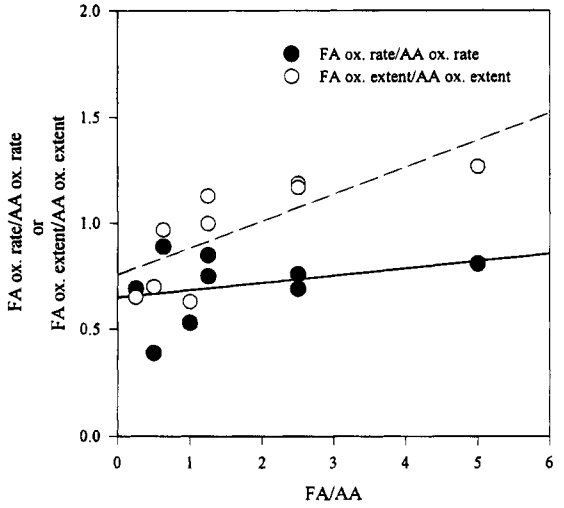

FIGURE 4: Effect of cosubstrate/fatty acid ratio on relative peroxidase and cyclooxygenase reaction rates and extents. PGHS holoenzyme (35 nM) was incubated at 25 °C in 0.1 M potassium phosphate (pH 8.0) with 20, 40, or 80 μM arachidonate and 20, 50, or 100 μM ferulate. The kinetics of ferulate oxidation (from A_{310} measurements) and arachidonate oxygenation (from oxygen measurements) were monitored in parallel reactions, in duplicate, for each combination of arachidonate and ferulate concentrations. Arachidonate oxygenation rates were corrected for oxygen electrode membrane damping by using the standard curve in the inset to the lower panel of Figure 3 and assumed a stoichiometry of 1 mol of arachidonate oxygenated/2 mol of oxygen consumed. The ratios of the average peak rates (●) and the average extents at 30 s (○) are plotted as functions of the ratio of the initial ferulate and arachidonate levels. Lines were fitted to the points by linear regression. Details are described in the text and in Materials and Methods.

(average of 0.71). The rates ratio increased only slightly as the initial cosubstrate/fatty acid ratio was increased from 0.25 to 5.0 (Figure 4). These observations show that the peak rate of PGG_2 formation was considerably greater than the peak rate of cosubstrate oxidation under all of the conditions examined.

Comparison of Cumulative Extents of Ferulate Oxidation and Arachidonate Oxygenation. The peak peroxidase and cyclooxygenase catalytic rates need not be representative of the rates at other points during the reactions. Ferulate oxidation and arachidonate oxygenation were almost complete after 30 s (Figure 3), so that the reaction extents at 30 s provide an integrated measure of the peroxidase and cyclooxygenase rates over essentially the whole reaction. Measurement of the reaction extents also is less sensitive to the effects of differences in cuvette geometry and mixing dynamics between the spectrophotometric and polarographic assays than is measurement of the reaction velocities at the early peak point. The observed ratios of the peroxidase and oxygenase extents ranged from 0.63 to 1.27 and appeared to increase linearly with the substrate ratio (Figure 4). The peroxidase/oxygenase ratios calculated from reaction extents at 30 s were generally higher than the corresponding ratios calculated from peak reaction rates (Figure 4). Because the extents are integrated rates, this difference indicates that the ratio between the peroxidase and oxygenase rates varied over the course of the reaction.

Peroxidase Self-Inactivation. The extent of inactivation of PGHS peroxidase capacity after prolonged reaction with arachidonate was assessed from the amount of cosubstrate oxidation that occurred upon the addition of 15-HPETE, a

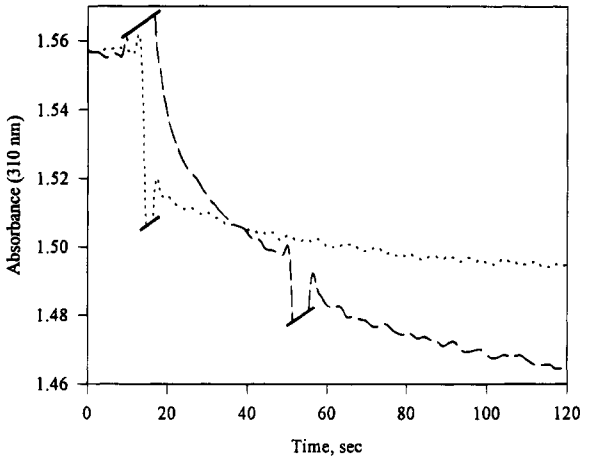

FIGURE 5: Inactivation of peroxidase capacity during reaction of PGHS with arachidonate. PGHS holoenzyme (35 nM) in 0.1 M potassium phosphate (pH 8.0) with 100 μM ferulate at 25 °C was reacted with 20 μM 15-HPETE alone (• • •) or with 80 μM arachidonate for 30 s before the addition of 20 μM 15-HPETE (- - -). Oxidation of ferulate was monitored from absorbance changes at 310 nm. The spikes in the traces produced during reagent addition have been truncated for clarity.

lipid hydroperoxide. In the presence of ferulate, the addition of 15-HPETE after 30 s of reaction with arachidonate produced a secondary burst of ferulate oxidation that was 22% as large as that produced in the control reaction without arachidonate (Figure 5). The initial absorbance change after 30 s of reaction with arachidonate corresponds to the oxidation of only 8 μM ferulate, so that the cosubstrate and fatty acid levels were not limiting at any point. The bulk of the peroxidase thus was inactivated early in the reaction of PGHS with arachidonate and ferulate, which may explain the persistence of PGG_2 at later times in such reactions (Figure 2C).

Reaction simulations. Some distinguishing kinetic characteristics of the branched-chain and tightly coupled mechanisms are not readily apparent from simple inspection of the mechanistic forms in Schemes 1 and 2. Reaction simulations with reasonable values for individual rate constants were used to obtain approximate predictions of the kinetics expected from the branched-chain and tightly coupled mechanisms (Materials and Methods). Under conditions of excess arachidonate and ferulate and catalytic amounts of enzyme, the oxygen consumption predicted by the branched-chain mechanism accelerated quickly, reaching a maximal rate of 3.7 μM O_2 s^{-1} within 1−2 s (Figure 6A). The predicted decreases in arachidonate and ferulate levels paralleled the oxygen consumption, and both PGG_2 and PGH_2 accumulated. To simplify matters, the basic simulations did not include any self-inactivation process. Because of this, the cumulative product levels predicted were unrealistically high (compare Figure 6A with Figure 2C). Inclusion of a rudimentary self-inactivation process [Fe(IV)-Tyr• → inactive enzyme] with a first-order rate constant set at the experimentally observed value of 0.42 s^{-1} resulted in the prediction of realistic consumption of arachidonate and correspondingly lower product levels (Figure 6C).

With the same initial conditions (excess arachidonate and ferulate and catalytic amounts of enzyme), kinetic simulation based on the tightly coupled mechanism predicted unrealistically low rates of oxygen, arachidonate, and ferulate consumption (Figure 6B). To confirm our expectation that

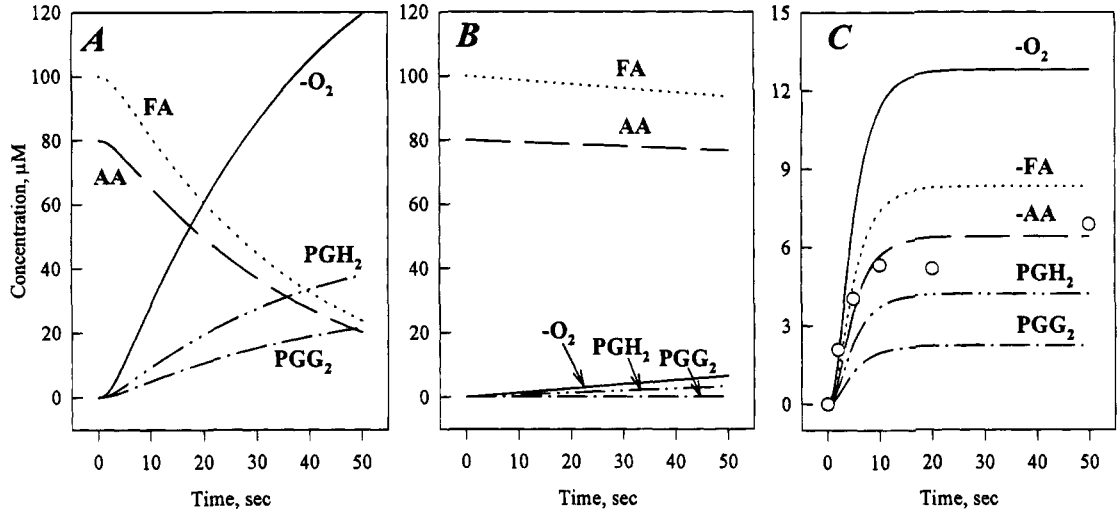

FIGURE 6: Simulation of reaction kinetics with a catalytic level of PGHS. Changes in the levels of substrates and products during reaction of 35 nM PGHS with 80 μM arachidonate and 100 μM FA were simulated for either the branched-chain (panel A) or the tightly coupled (panel B) mechanism without self-inactivation or for the branched-chain mechanism with a self-inactivation step (panel C). In each case, the initial hydroperoxide concentration was set at 20 nM, the continuous level needed to sustain half-maximal cyclooxygenase activation experimentally (Kulmacz & Lands, 1983). The simulation procedure is described in Materials and Methods.

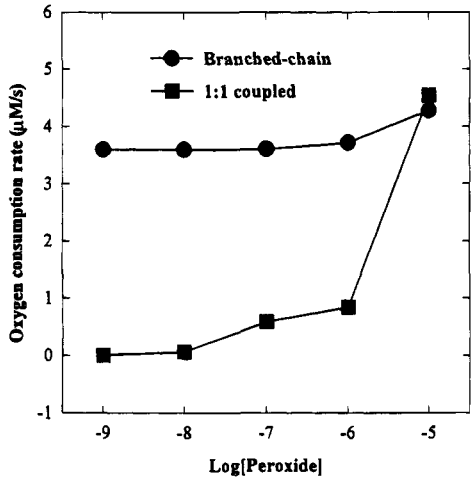

FIGURE 7: Effect of the initial hydroperoxide level on the peak cyclooxygenase velocities predicted by the branched-chain (●) and tightly coupled (■) mechanisms. Reactions of catalytic levels of PGHS (35 nM) with 80 μM arachidonate, 100 μM FA, and the indicated initial hydroperoxide concentrations were simulated as described in the legend to Figure 6.

this low predicted activity was a consequence of the low initial hydroperoxide level, the simulation for the tightly coupled mechanism was repeated to predict the maximal oxygen consumption rate with initial hydroperoxide levels ranging between 10^{-9} and 10^{-5} M. As can be seen from the results in Figure 7, the cyclooxygenase rate predicted for the tightly coupled mechanism reached an appreciable value only when the hydroperoxide was well above 10^{-6} M. In contrast, the maximal cyclooxygenase rate predicted in parallel simulations for the branched-chain mechanism was relatively independent of the initial hydroperoxide level (Figure 7). The two mechanisms led to similar predicted cyclooxygenase rates with initial hydroperoxide levels near 10^{-5} M.

The response of the cyclooxygenase rate to increases in the initial hydroperoxide level was examined experimentally in reactions where 100 μM ferulate, 0−10 μM 15-HPETE, and 80 μM arachidonate were added sequentially before injection of 14 nM PGHS. The cyclooxygenase rate was found to be decreased by the addition of 15-HPETE, reaching 78% of the control with 1 μM 15-HPETE and 53% of the control with 10 μM 15-HPETE. There was no indication of the large stimulatory effect of micromolar levels of hydroperoxide on the cyclooxygenase activity that was predicted by the tightly coupled mechanism (Figure 7). The observed decrease in activity presumably reflects rapid hydroperoxide-dependent inactivation with these relatively high hydroperoxide levels (Markey et al., 1987). For simplicity, hydroperoxide-dependent inactivation was not included in kinetic simulations with either mechanism.

Reactions of PGHS with stoichiometric levels of arachidonate in the absence of added cosubstrate were also simulated with the branched-chain and the tightly coupled mechanisms. Similar reaction conditions have been used to compare the kinetics of tyrosyl radical formation and cyclooxygenase activity (Tsai et al., 1992). Purified PGHS contains about 5−10 equiv of unidentified endogenous reductant, as evidenced by the ability of the homogeneous protein to produce PGH_2 in the absence of added cosubstrate (Tsai et al., 1992). This amount of reductant is negligible for reactions with catalytic levels of enzyme, but becomes a significant factor when the enzyme concentration approaches that of the fatty acid, especially in the absence of added peroxidase cosubstrate. Accordingly, the initial conditions for these simulations included 5 equiv of endogenous reductant. The kinetic simulations are shown in Figure 8. The cyclooxygenase reaction is predicted to occur very rapidly for the branched-chain mechanism (Figure 8A), with quantitative conversion of the fatty acid to PGG_2 and PGH_2 within 5 s. The formation of oxidized enzyme intermediates is also predicted to be rapid with the branched-chain mechanism (Figure 8C), with the sustained accumulation of the tyrosyl radical species [Fe(IV)Tyr•] and lower levels of compound II [Fe(IV)]. In contrast, the tightly coupled mechanism predicts very little consumption of arachidonate or oxygen and little accumulation of endoperoxides or oxidized enzyme intermediates over a comparable time frame (Figure 8B,D).

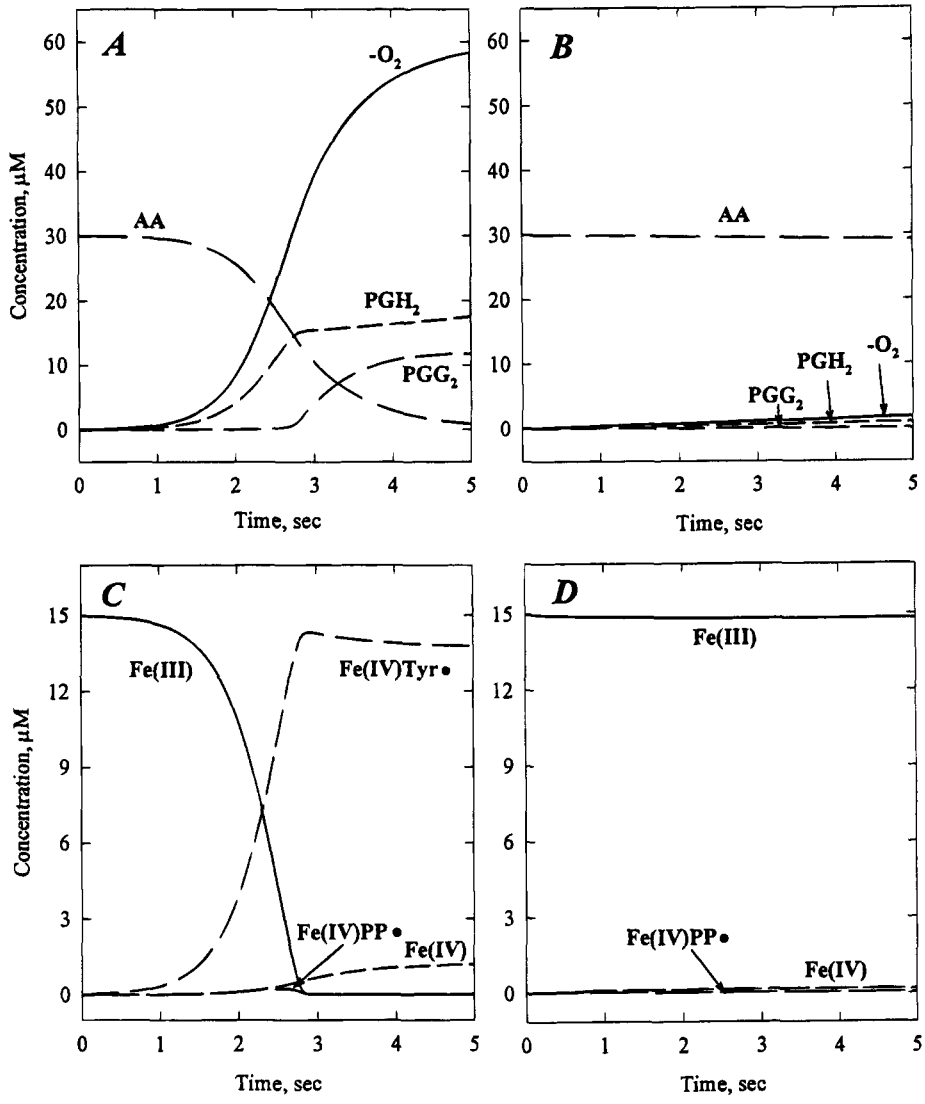

FIGURE 8: Simulation of reaction kinetics with stoichiometric levels of PGHS and arachidonate. Panels A and C are from a simulation with the branched-chain mechanism using 30 μM AA, 15 μM PGHS, and initial peroxide at 3×10^{-8} M. Panels B and D are from a simulation with the tightly coupled mechanism using the same initial conditions. Panels A and B show the predicted changes in levels of substrates and products, whereas panels C and D show the predicted levels of enzyme intermediates (see Schemes 1 and 2). Cosubstrate was not included, but the enzyme was assumed to contribute an endogenous reductant level of 75 μM. All rate constants were decreased from the values in Tables 1 and 2 to reflect a temperature of 0 °C. The endogenous reductant was assumed to undergo the same reactions as ferulate at one-fiftieth of the rate. Details of the simulation procedure are described in Materials and Methods.

DISCUSSION

A summary of the observed PGHS reaction characteristics and those predicted by the branched-chain and tightly coupled mechanisms is presented in Table 4. A detailed discussion of how well the two mechanisms account for individual aspects of observed cyclooxygenase and peroxidase reaction kinetics is given here.

Accumulation of PGG_2. Initiation of cyclooxygenase catalysis in the branched-chain mechanism (k_1 and k_2 in Scheme 1) requires a 2-electron oxidation by hydroperoxide, but the cyclooxygenase propagation reactions (k_3, k_4, and k_5 in Scheme 1) do not involve changes in the net oxidation state, as the unpaired electron is simply transferred from the tyrosyl radical to the bound substrate/product and then back to the tyrosine. Thus, many rounds of cyclooxygenase catalysis can occur before the reactive intermediate is quenched by reducing cosubstrate (k_7). In the tightly coupled mechanism, cyclooxygenase initiation also requires a 2-electron oxidation by hydroperoxide (k_1 in Scheme 2). However, two obligatory 1-electron reductions by cosubstrate (k_5 and k_6) occur before the catalytic cycle is complete, leaving the enzyme in the resting state. This requires that the cyclooxygenase be reinitiated after every round of catalysis.

As a result of the fundamental differences in the need for cyclooxygenase reinitiation, the branched-chain and tightly coupled mechanisms predict very different fates for PGG_2 produced from arachidonate oxygenation. In the branched-chain mechanism, PGG_2 is released at the end of each cyclooxygenase cycle, and its consumption is essentially independent of further cyclooxygenase catalysis. In the tightly coupled mechanism, the PGG_2 produced in one cycle of cyclooxygenase catalysis is completely consumed in reactivating the enzyme for the next catalytic cycle. Thus, the branched-chain mechanism allows for the accumulation of PGG_2, whereas the tightly coupled mechanism does not. It must be emphasized once again that this distinction in the predicted ability to accumulate PGG_2 is a consequence of

Table 4: Summary of Predicted and Observed PGHS Reaction Characteristics

characteristic	prediction[a]		experimental observation
	branched-chain mechanism	tightly coupled mechanism	
PGG_2 accumulation in presence of cosubstrate	yes	no	yes[b]
cosubstrate/fatty acid consumption stoichiometry	between 0 and 2	exactly 2	0.6−1.3[c]
initial [hydroperoxide] required for cyclooxygenase activity	$<10^{-9}$ M	$>10^{-6}$ M	$<10^{-8}$ M[d]
early cyclooxygenase kinetics	acceleration after initial lag	linear with no lag	acceleration after initial lag[e]
higher oxidation states in reaction with arachidonate	detectable	probably not detectable	detectable[f]
sensitivity to inhibition by cyanide	peroxidase > cyclooxygenase	peroxidase = cyclooxygenase	peroxidase > cyclooxygenase[g]
sensitivity to inhibition by glutathione peroxidase	peroxidase > cyclooxygenase[h]	peroxidase = cyclooxygenase	peroxidase > cyclooxygenase[i]
cosubstrate required for cyclooxygenase activity	no	yes	no[j]
effect of increased [cosubstrate] on cyclooxygenase activity	inhibitory only	stimulatory only	biphasic[k]

[a] Predictions are based on the form of the mechanisms in Schemes 1 and 2 or on kinetic simulations based on those mechanisms, except as indicated. [b] Figure 2 in present study; Kulmacz, 1987; Eling et al., 1991. [c] Figure 4 in present study. [d] The initial [hydroperoxide] required will be less than the 20 nM needed to *sustain* cyclooxygenase reaction (Kulmacz & Lands, 1983). [e] Initial lag and acceleration in corrected oxygenase velocity are more apparent with TMPD as cosubstrate (Kulmacz, 1987). [f] Lambeir et al., 1985; Dietz et al., 1988; MacDonald & Dunford, 1989; Tsai et al., 1992. [g] Hemler & Lands, 1980; Kulmacz & Lands, 1985. [h] Kulmacz et al., 1994. [i] Kulmacz & Lands, 1983. [j] Added cosubstrate is not required (Miyamoto et al., 1976; van der Ouderaa et al., 1977; Hemler et al., 1978). Note that purified PGHS does contain some endogenous reductant. [k] Lands & Hanel, 1983.

the forms of the two mechanisms and does not require precise knowledge of the values of individual rate constants.

Analysis of the arachidonate metabolite kinetics provided direct evidence for the accumulation of PGG_2 during reaction of PGHS with fatty acid in the presence of added reducing cosubstrate (Figure 2). The peak level of PGG_2 actually increased in the presence of cosubstrate, increasing from about 0.7 μM in the control (Figure 2A) to about 1.2 μM with 100 μM FA (Figure 2C) and about 2.3 μM with 1 mM phenol (Figure 2E). These increases in the peak PGG_2 level suggest that the cosubstrates actually stimulated the rate of PGG_2 production more than the rate of PGG_2 removal. Detectable PGG_2 accumulated even in the presence of 5 mM phenol (Figure 2F), a cosubstrate level that inhibited the cyclooxygenase velocity by about 50% from the peak value obtained with 1 mM phenol. The demonstration that PGG_2 accumulates even in the presence of cosubstrate is entirely consistent with the branched-chain mechanism, but contradicts the tightly coupled mechanism.

The persistence of near-peak levels of PGG_2 after 50 s of incubation in the presence of excess substrate and cosubstrate (Figure 2B−F) suggested that both the peroxidase and cyclooxygenase activities became inactivated. Substantial self-inactivation of the peroxidase was confirmed by the observation that only a small fraction of residual FA oxidation was triggered by the addition of exogenous hydroperoxide after most arachidonate metabolism had ceased (Figure 5). This loss of 80% of the hydroperoxide-dependent FA oxidation capacity contrasted with the retention of about 70% of the hydroperoxide-dependent TMPD oxidation capacity under similar circumstances (Kulmacz, 1987). Apparently, the self-inactivated enzyme is still capable of oxidizing TMPD in a hydroperoxide-dependent process unrelated to normal peroxidase reduction of PGG_2 to PGH_2.

There have been some reports that PGG_2 accumulates in the presence of cosubstrate (Kulmacz, 1987; Eling et al., 1991), and other reports that only PGH_2 is found (Egan et al., 1976; Miyamoto et al., 1976; Graff, 1982; Hecker et al., 1987). The apparent contradiction between these observations can be explained by differences in reaction conditions, in particular whether the enzyme or the substrate is limiting. When the enzyme is limiting, as indicated by the presence of unreacted fatty acid, the peroxidase is self-inactivated at about the same time as the cyclooxygenase (Figures 3 and 5), before all of the PGG_2 can be converted to PGH_2. Reactions under these conditions seem to result in the accumulation of PGG_2 itself (Figure 2; Kulmacz, 1987) or PGG_2 degradation products (Eling et al., 1991). If the substrate is limiting, as indicated by observed consumption of most of the fatty acid (Egan et al., 1976; Miyamoto et al., 1976; Graff, 1982; Hecker et al., 1987), the rate of PGG_2 production slows due to exhaustion of the fatty acid rather than self-inactivation. Any accumulated PGG_2 (or PGG_1) would be expected to be reduced rather quickly to PGH_2 (or PGH_1) by the surviving peroxidase activity under these conditions. Thus, these reports of PGH_2 accumulation do not preclude an earlier, transient accumulation of PGG_2.

Evaluation of Fatty Acid Oxygenation Rate. The value of the ratio of the peak peroxidase and cyclooxygenase velocities has been cited as proving that PGHS catalysis proceeds via the tightly coupled mechanism and ruling out a branched-chain mechanism (Bakovic & Dunford, 1994). Thus, the procedures for evaluating cosubstrate oxidation and fatty acid oxygenation need to be considered carefully. Ferulic acid is a convenient substrate as its oxidation can be accurately measured spectrophotometrically, and oxidized ferulate does not undergo further reaction with oxygen (Bakovic & Dunford, 1994). Measurement of arachidonate oxygenation is more complicated. Accurate measurements of rapid oxygen uptake kinetics require correction of the electrode response for the damping effect of the electrode membrane (Cook et al., 1979). In the present study, the actual oxygenase velocity was almost twice that of the uncorrected electrode signal (Figure 3, lower panel). Bakovic and Dunford (1994) used uncorrected oxygen electrode signals to calculate the arachidonate oxygenation rate. As a result, their values for the cyclooxygenase rates probably

need to be revised upward by a factor of approximately 2.

The issue of oxygenase activity in the absence of added cosubstrate also needs to be considered. The tightly coupled mechanism does not admit activity without cosubstrate (Scheme 2), and the oxygenase activity observed in the absence of added cosubstrate was considered a spontaneous background to be subtracted from the total activity (Bakovic & Dunford, 1994). However, oxygenase activity in the absence of added cosubstrate is not negligible, as it ranges from 20 to 60% of the maximal activity observed in the presence of added cosubstrate, depending on the cosubstrate and the reaction conditions (Hemler & Lands, 1980; Kulmacz & Lands, 1985; Hsuanyu & Dunford, 1992; Results). Also, addition of ferulate or phenol did not alter the arachidonate metabolites produced (just their proportions) (Figure 1; Graff, 1982), nor did the addition of cosubstrate appreciably change the K_m for arachidonate (Hemler et al., 1978). These observations indicate that the oxygenase activity observed without added cosubstrate reflects cyclooxygenase-catalyzed synthesis of the normal prostaglandin endoperoxide and not a spurious background. It thus seems reasonable to include all of the cyclooxygenase activity in calculations of the ratio of ferulate oxidation to arachidonate oxygenation, as has been done in the present study.

Stoichiometry between Cosubstrate Oxidation and Fatty Acid Oxygenation. The ratio between cosubstrate and fatty acid consumption provides a measure of the degree to which the peroxidase and cyclooxygenase catalytic cycles are coupled to one another at a given time in the reaction. The forms of the two mechanisms (Schemes 1 and 2) lead to very different predictions for the value of the peroxidase/cyclooxygenase ratio; thus, the ratio furnishes a useful way to test the mechanisms. For the tightly coupled mechanism (Scheme 2), each cycle of cyclooxygenase catalysis requires completion of a cycle of peroxidase catalysis, so that the rates of the two cycles are always in fixed proportion. Cosubstrate participates in two steps (k_5 and k_6 in Scheme 2) and fatty acid in only one (k_2 in Scheme 2), so that the ratio of cosubstrate and arachidonate consumption is exactly 2 in this mechanism. For the branched-chain mechanism, propagation of the cyclooxygenase reaction (k_3, k_4, and k_5 in Scheme 1) does not require further peroxidase catalysis, so that the peroxidase and cyclooxygenase velocities need not be in any fixed ratio.

In the present experiments, the peak rate of ferulate oxidation in each case was less than that of arachidonate oxygenation, with the ratio between the two rates averaging 0.71 (Figure 4). When the total oxygenase rates obtained by Bakovic and Dunford (1994) are corrected by a factor of 1.8 to account for the electrode membrane damping (Figure 3, lower panel), their peroxidase/oxygenase ratios average about 0.7. Thus, the present rate ratios based on total oxygenase agree well with those of Bakovic and Dunford (1994). Because complete conversion of PGG_2 to PGH_2 requires 2 equiv of reductant, these observations of rate ratios of 0.7 indicate that, at the peak of the reaction, PGG_2 was being reduced to PGH_2 by the peroxidase much more slowly than it was being generated from arachidonate by the cyclooxygenase. This is consistent with the branched-chain mechanism, but contradicts the tightly coupled mechanism.

The observed ratio between the peak peroxidase and cyclooxygenase rates changed little as the initial cosubstrate/substrate ratio increased by 20-fold, from 0.25 to 5.0 (Figure 4). This suggests that some sort of kinetic linkage does exist between the two catalytic activities. Unlike the tightly coupled mechanism, where the cyclooxygenase and peroxidase cycles are fused (Scheme 2), the branched-chain mechanism (Scheme 1) lacks a direct kinetic linkage between the two activities once the cyclooxygenase has been initiated (via the k_2 step). However, an increase in the cyclooxygenase rate tends to raise the PGG_2 level, and this itself would increase the peroxidase activity. This indirect linkage of the peroxidase and cyclooxygenase via PGG_2 may well account for the observation of roughly proportionate changes in the two catalytic rates (Figure 4).

The ratio between cumulative cosubstrate and fatty acid consumption provides a second check on the degree of coupling between peroxidase and cyclooxygenase catalysis and an independent way to determine whether significant PGG_2 remained at the end of the reaction. The tightly coupled mechanism requires that all PGG_2 produced be converted to PGH_2, thus giving a stoichiometry of exactly 2 mol of cosubstrate/mol of fatty acid at all points in the reaction (Bakovic & Dunford, 1994). The branched-chain mechanism allows the peroxidase to work independently of the activated cyclooxygenase, which permits any stoichiometry between essentially 0 (if no further PGG_2 is consumed after initiation) and 2 (if all of the PGG_2 is eventually converted to PGH_2 by the peroxidase).

In the actual experiments, the ratio of the extents of ferulate oxidation and arachidonate oxygenation at 30 s, when the reactions were largely complete, did not exceed 1.3 (Figure 4), which is well below the stoichiometry of 2 required by the tightly coupled mechanism, but within the range of 0−2 predicted by the branched-chain mechanism. Conversion of PGG_2 to PGH_2 consumes 2 equiv of reductant, regardless of the reaction mechanism. Because no more than 1.3 mol of cosubstrate was actually oxidized per mole of arachidonate oxygenated during the reaction, some of the oxygenated arachidonate (i.e., PGG_2) was not reduced by the peroxidase and remained intact. Thus, the extent ratios (Figure 4) confirm the direct observation of PGG_2 accumulation in the presence of cosubstrate (Figure 2). It is interesting to note that the 30 s peroxidase/oxygenase extent ratio calculated by using the peroxidase and total oxygenase data in Figure 4 of Bakovic and Dunford (1994) is approximately 0.9, indicating that PGG_2 probably accumulated in that reaction.

Overall, the observed stoichiometry between cosubstrate oxidation and fatty acid oxygenation, no matter whether calculated from peak rates or cumulative reaction extents, clearly shows that the peroxidase and cyclooxygenase catalytic cycles are not tightly coupled. This conclusion is consistent with the branched-chain mechanism (Scheme 1), but contradicts a central hypothesis implicit in the tightly coupled mechanism (Scheme 2).

Sensitivity of the Cyclooxygenase to the Initial Hydroperoxide Level. Activation of the cyclooxygenase has long been known to require hydroperoxide (Smith & Lands, 1972). The effects of changes in hydroperoxide activator level are not apparent from the tightly coupled and branched-chain mechanisms (Schemes 1 and 2); thus, kinetic simulations were employed (Figure 7). The branched-chain and tightly coupled mechanisms predicted very different responses of the cyclooxygenase velocity to increases in the initial hydroperoxide level. This difference is particularly pronounced at initial hydroperoxide levels below 10^{-6} M, where

only the branched-chain mechanism predicted appreciable cyclooxygenase activity. The branched-chain mechanism in fact predicted appreciable cyclooxygenase velocities, even when the starting hydroperoxide level was below 10^{-9} M (Figure 7). This predicted initial hydroperoxide requirement is well below the 20 nM level of hydroperoxide that must be continuously present to sustain half-maximal cyclooxygenase velocity (K_p value) (Kulmacz & Lands, 1983). There is no contradiction between these values because the branched-chain mechanism predicts that PGG_2 can accumulate from very low starting levels to levels near the K_p value in a matter of seconds.

In the present study, the arachidonate stock was pretreated with borohydride to decompose hydroperoxides and a small level of BHT was added (Kulmacz & Lands, 1987), but no other steps were taken to suppress later hydroperoxide formation in the working fatty acid solution. Although unlikely, it is conceivable that enough autoxidation of the fatty acid may have occurred under the present conditions to raise the initial hydroperoxide to the 10^{-6} M range predicted to be required for effective cyclooxygenase activity with the tightly coupled mechanism (Figure 7). However, cyclooxygenase activity was not appreciably blunted even when the fatty acid was continuously treated with glutathione peroxidase until immediately before use to prevent hydroperoxide accumulation (Kulmacz et al., 1994). Only when large levels of glutathione peroxidase are present in the PGHS reaction itself does the cyclooxygenase velocity become inhibited (Kulmacz & Lands, 1983; Odenwaller et al., 1993; Kulmacz et al., 1994). Further, the cyclooxygenase activity was not increased when the initial hydroperoxide level was augmented with 1−10 μM 15-HPETE (Results). The ability of the cyclooxygenase reaction to start with very low initial hydroperoxide levels seems much more consistent with the characteristics of the branched-chain mechanism, which allows PGG_2 accumulation as the reaction progresses, than with those of the tightly coupled mechanism, which restricts the hydroperoxide level to that initially present (Figures 6 and 7).

Initial Cyclooxygenase Kinetics. Cyclooxygenase catalysis by PGHS is characterized by an initial lag and an accelerative early phase. The lag and acceleration of the oxygenase activity were not observed with ferulate as the cosubstrate due to instrumental limitations (Fig. 3), but they become readily apparent with other cosubstrates, such as TMPD (Kulmacz, 1987). Cyclooxygenase acceleration reflects a positive feedback loop involving the product hydroperoxide, as is evident from the longer lags and slower acceleration observed when PGG_2 is continuously decomposed by added glutathione peroxidase (Hemler & Lands, 1980). Positive feedback is expected from the branched-chain mechanism in Scheme 1 because PGG_2 formed by one PGHS molecule can accumulate and initiate cyclooxygenase catalysis of other PGHS molecules. The curvature in the first 1−2 s of the predicted oxygen consumption trace in Figure 6A reflects the increasing velocity as all of the PGHS gradually becomes activated. On the other hand, positive feedback is not expected from the tightly coupled mechanism in Scheme 2 because the PGG_2 produced in one catalytic cycle is consumed to activate the enzyme for the next cycle. The contaminant hydroperoxide initially present does initiate cyclooxygenase catalysis by a stoichiometric amount of the enzyme, but no net production of hydroperoxide occurs and the fraction of activated enzyme cannot increase. The lack of an accelerative phase is clear in the oxygen consumption trace predicted with the tightly coupled mechanism (Figure 6B). Thus, the branched-chain mechanism, but not the tightly coupled mechanism, can account for the accelerative kinetics characteristic of cyclooxygenase catalysis by PGHS.

Generation of Higher Oxidation State Intermediates. Spectrophotometric observations indicate that a considerable portion of the PGHS heme is in the ferryl oxidation state during reaction of the enzyme with arachidonate (Lambeir et al., 1985; Dietz et al., 1988; MacDonald & Dunford, 1989). EPR observations during similar reactions demonstrate the formation of tyrosyl radical species whose kinetics seem to correlate with those of the optical signals from ferryl heme (Karthein et al., 1988; Tsai et al., 1992). This indicates that the major intermediates during reaction of PGHS with arachidonate in the absence of added cosubstrate correspond to Fe(IV)Tyr• and Fe(IV) in the branched-chain mechanism (Scheme 1) or Fe(IV) in the tightly coupled mechanism (Scheme 2). Compound I [Fe(IV)PP• in Schemes 1 and 2] presumably is formed transiently in these reactions with arachidonate, but does not reach detectable levels (Lambeir et al., 1985; Dietz et al., 1988; MacDonald & Dunford, 1989).

Simulations of reactions of PGHS with limiting arachidonate in the absence of added cosubstrate, under conditions comparable to those used for the spectroscopic studies, have been done with both the branched-chain and tightly coupled mechanisms (Figure 8). The levels of oxidized intermediates were predicted to rise to easily detectable fractions of total enzyme only with the branched-chain mechanism (compare panels C and D in Figure 8). This reflects the predicted ability of the branched-chain mechanism, but not the tightly coupled mechanism, to accumulate PGG_2 above the initial level of contaminant hydroperoxide (Figure 8, panels A and B). The branched-chain mechanism predicts a sustained accumulation of Fe(IV)Tyr•, and later Fe(IV), that is quite consistent with the optical and EPR observations (Lambeir et al., 1985; Dietz et al., 1988; Karthein et al., 1988; MacDonald & Dunford, 1989; Tsai et al., 1992). The predicted peak level of Fe(IV)Tyr• (Figure 8C) is higher than that observed by EPR (Tsai et al., 1992), probably because self-inactivation was not included in the simulation. Thus, the observed formation of oxidized enzyme intermediates can be more readily accounted for by the branched-chain mechanism than by the tightly coupled mechanism.

Differential Inhibition of Cyclooxygenase and Peroxidase Activities. The peroxidase activity of PGHS has been found to be much more sensitive than the cyclooxygenase activity to inhibition by the heme ligand, cyanide, and by the hydroperoxide scavenger, glutathione peroxidase (Hemler & Lands, 1980; Kulmacz & Lands, 1983, 1985). This differential inhibition of the two activities is very difficult to reconcile with the tightly coupled mechanism, where the cyclooxygenase and peroxidase cycles are fused in such a manner that inhibition of one activity would necessarily inhibit the other by the same amount (Scheme 2). On the other hand, propagation of the cyclooxygenase and the peroxidase are essentially independent processes in the branched-chain mechanism (Scheme 1), so that differential inhibition of two activities can be accommodated. Additional simulations with the branched-chain mechanism in Scheme 1 (data not shown) or with a similar branched-chain mechanism (Kulmacz et al., 1994) predict that it is the

peroxidase activity that is more readily inhibited by cyanide or glutathione peroxidase, which is in line with the experimental observations (Hemler & Lands, 1980; Kulmacz & Lands, 1983, 1985). Also, the primary effect of cyanide in the branched-chain mechanism is on the initiation of the cyclooxygenase via the k_1 step (Scheme 1). This agrees well with the observation that increasing cyanide binding to the PGHS heme coincided with decreasing cyclooxygenase initiation efficiency (Kulmacz & Lands, 1985).

Effects of Cosubstrates on Cyclooxygenase Activity. As already mentioned, purified PGHS is capable of cyclooxygenase catalysis in the absence of added peroxidase cosubstrates (Miyamoto et al., 1976; van der Ouderaa et al., 1977; Hemler et al., 1978). Cyclooxygenase catalysis in the branched-chain mechanism does not require reducing cosubstrates (Scheme 1), whereas two reactions with reductant are integral parts of cyclooxygenase catalysis in the tightly coupled mechanism (the k_5 and k_6 steps in Scheme 2). However, the tightly coupled mechanism cannot be ruled out on this basis because homogeneous PGHS itself has some reductant. The presence of this endogenous reductant is evident from the conversion of arachidonate to both PGG_2 and PGH_2 and from the decay of oxidized peroxidase intermediates, even when care is taken to exclude potential reductants from the reaction (Dietz et al., 1988; Kulmacz et al., 1990; Tsai et al., 1992). The endogenous reductant is not removed by chromatography, nor is it consumed by treatment with mild oxidant, such as ferricyanide,[3] suggesting that moderately labile amino acid residues of the protein itself may be involved. Whatever its identity, the endogenous reductant could conceivably furnish the reducing equivalents required for cyclooxygenase catalysis in the tightly coupled mechanism.

Many substances that act as peroxidase cosubstrates have biphasic effects on the cyclooxygenase activity, with stimulatory actions at lower levels and inhibitory actions at higher levels (Lands & Hanel, 1983). A quantitative examination of the effects of the cosubstrate structure on this biphasic behavior has been done for a series of phenolic compounds, with the actions of the compounds rationalized in terms of distinct electronic and hydrophobic interactions with the protein (Hsuanyu & Dunford, 1992). The complex effects of peroxidase cosubstrates are not well explained by either of the basic mechanisms under consideration, as is described in the following.

The tightly coupled mechanism in Scheme 2 predicts a saturable stimulation of the cyclooxygenase as the cosubstrate level is increased, but no inhibition (data not shown). An earlier version of the tightly coupled mechanism (Hsuanyu & Dunford, 1992) postulated competition between the cosubstrate and the fatty acid for reaction with compound I as the cause of cyclooxygenase inhibition, but this step was not included in the later formulation of the mechanism (Bakovic & Dunford, 1994) and it was accordingly omitted from the mechanism in Scheme 2. Addition of a reduction of compound I by cosubstrate to the mechanism in Scheme 2 clearly would have an inhibitory effect on cyclooxygenase activity and might well result in an overall biphasic response to cosubstrate. However, the cyclooxygenase velocities predicted by the tightly coupled mechanism in Scheme 2 at moderate initial hydroperoxide levels are already very low (Figures 6 and 7), and an additional inhibitory influence of cosubstrate would lead to even less realistic predictions of the cyclooxygenase velocity.

The branched-chain mechanism in Scheme 1 does predict the inhibitory effect of cosubstrates on the cyclooxygenase activity, but not the stimulatory effect (data not shown). This is one instance where predictions from this branched-chain mechanism did not fit well with experimental observations (Table 4), indicating that some important reactions of cosubstrate with the enzyme were not included in Scheme 1. Several possibilities remain to be investigated. A catalytic action in a cyclooxygenase step has been proposed (Kulmacz et al., 1994) on the basis of the observation that tryptophan stimulates the cyclooxygenase without being oxidized itself (Ohki et al., 1979). Reaction of cosubstrate with $PGG_2^{\bullet}$, a step in the tightly coupled mechanism (Scheme 2), is another way that cyclooxygenase velocity might be increased. The effect of cosubstrates on the cyclooxygenase remains a characteristic of PGHS behavior that lacks a satisfying biochemical explanation.

Structural Implications of the Reaction Mechanisms. Recent crystallographic data (Picot et al., 1994) have confirmed a previous conclusion from kinetic results (Marshall & Kulmacz, 1988) that PGHS has separate peroxidase and cyclooxygenase active sites. The presence of distinct sites is quite consistent with the variable ratio between peroxidase and cyclooxygenase activities that is predicted by the branched-chain mechanism and observed experimentally (Figure 4). In addition, Tyr385 is interposed between and abuts the peroxidase and cyclooxygenase sites in the PGHS structure (Picot et al., 1994). Tyr385 has been shown to be essential for cyclooxygenase activity and for generation of the native tyrosyl radical species (Shimokawa et al., 1990; Tsai et al., 1994). The native tyrosyl radical has been shown to be kinetically competent (Tsai et al., 1992) and to oxidize arachidonate to a fatty acyl radical (Tsai et al., 1995), consistent with the role of the radical in the branched-chain mechanism (Scheme 1). Thus, the structure of PGHS, with a competent oxidizing residue interposed between the peroxidase and cyclooxygenase sites, fits very well with the elements of the branched-chain mechanism.

In contrast, the crystal structure has no obvious internal channel that might ensure efficient transfer of PGG_2 from the cyclooxygenase site to the peroxidase site, nor does occupation of the cyclooxygenase site pose any obvious impediment to the access of hydroperoxide to the peroxidase site (Picot et al., 1994). As a consequence, it is difficult to envision a physical basis for the rigid synchronization of cyclooxygenase and peroxidase activities that is required by the tightly coupled mechanism.

Summary. Qualitative and quantitative predictions from a branched-chain mechanism (Dietz et al., 1988) and a tightly coupled mechanism (Bakovic & Dunford, 1994) have been compared with several observed characteristics of the PGHS reaction with arachidonate, including accumulation of PGG_2 and oxidized enzyme intermediates, stoichiometry of cosubstrate and fatty acid consumption, and hydroperoxide activator requirement. The observed characteristics are largely consistent with predictions from the branched-chain mechanism, but contradict important predictions of the tightly coupled mechanism.

[3] A.-L. Tsai, unpublished results.

ACKNOWLEDGMENT

We thank Mr. Chris Walker for his help with purification of the enzyme.

REFERENCES

Bakovic, M., & Dunford, H. B. (1994) *Biochemistry 33*, 6475−6482.

Boudart, M. (1968) *Kinetics of Chemical Processes*, pp 124−136, Prentice-Hall, Englewood Cliffs, NJ.

Cook, H. W., Ford, G., & Lands, W. E. M. (1979) *Anal. Biochem. 96*, 341−351.

Dietz, R., Nastainczyk, W., & Ruf, H. H. (1988) *Eur. J. Biochem. 171*, 321−328.

Egan, R. W., Paxton, J., & Kuehl, F. A., Jr. (1976) *J. Biol. Chem. 251*, 7329−7335.

Eling, T. E., Glasgow, W. C., Curtis, J. F., Hubbard, W. C., & Handler, J. A. (1991) *J. Biol. Chem. 266*, 12348−12355.

Graff, G. (1982) *Methods Enzymol. 86*, 376−385.

Hamberg, M., & Samuelsson, B. (1967) *J. Biol. Chem. 242*, 5336−5343.

Hecker, M., Hatzelmann, A., & Ullrich, V. (1987) *Biochem. Pharmacol. 36*, 851−855.

Hemler, M. E., & Lands, W. E. M. (1980) *J. Biol. Chem. 255*, 6253−6261.

Hemler, M. E., Crawford, C. G., & Lands, W. E. M. (1978) *Biochemistry 17*, 1772−1779.

Hsuanyu, Y., & Dunford, H. B. (1992) *J. Biol. Chem. 267*, 17649−17657.

Hurst, J. S., Flatman, S., & McDonald-Gibson, R. G. (1987) in *Prostaglandins and Related Substances: A Practical Approach* (Benedetto, C., McDonald-Gibson, R. G., Nigam, S., & Slater, T. F., Eds.) pp 53−73, IRL Press, Washington, D.C.

Karthein, R., Dietz, R., Nastainczyk, W., & Ruf, H. H. (1988) *Eur. J. Biochem. 171*, 313−320.

Kulmacz, R. J. (1987) *Prostaglandins 34*, 225−240.

Kulmacz, R. J., & Lands, W. E. M. (1983) *Prostaglandins 25*, 531−540.

Kulmacz, R. J., & Lands, W. E. M. (1985) *Prostaglandins 29*, 175−190.

Kulmacz, R. J., & Lands, W. E. M. (1987) in *Prostaglandins and Related Substances: A Practical Approach* (Benedetto, C., McDonald-Gibson, R. G., Nigam, S., & Slater, T. F., Eds.) pp 209-227, IRL Press, Washington, D.C.

Kulmacz, R. J., Tsai, A.-L., & Palmer, G. (1987) *J. Biol. Chem. 262*, 10524−10531.

Kulmacz, R. J., Ren, Y., Tsai, A.-L., & Palmer, G. (1990) *Biochemistry 29*, 8760−8771.

Kulmacz, R. J., Pendleton, R. B., & Lands, W. E. M. (1994) *J. Biol. Chem. 269*, 5527-5536

Lambeir, A.-M., Markey, C. M., Dunford, H. B., & Marnett, L. J. (1985) *J. Biol. Chem. 260*, 14894−14896.

Lands, W. E. M., & Hanel, A. M. (1983) in *Prostaglandins and Related Substances* (Pace-Asciak, C., & Granstrom, E., Eds.) pp 203-223, Elsevier Science Publishers.

MacDonald, I. D., & Dunford, H. B. (1989) *Biochem. Cell. Biol. 67*, 301−305.

Markey, C. M., Alward, A., Weller, P. E., & Marnett, L. J. (1987) *J. Biol. Chem. 262*, 6266−6279.

Marshall, P. J., & Kulmacz, R. J. (1988) *Arch. Biochem. Biophys. 266*, 162−170.

Miyamoto, T., Ogino, N., Yamamoto, S., & Hayaishi, O. (1976) *J. Biol. Chem. 251*, 2629−2636.

Odenwaller, R., Maddipati, K. R., & Marnett, L. J. (1993) *J. Biol. Chem. 267*, 13863−13869.

Ohki, S., Ogino, N., Yamamoto, S., & Hayaishi, O. (1979) *J. Biol. Chem. 254*, 829-836.

Picot, D., Loll, P. J., & Garavito, R. M. (1994) *Nature 367*, 243−249.

Shimokawa, T., Kulmacz, R. J., DeWitt, D. L., & Smith, W. L. (1990) *J. Biol. Chem. 265*, 20073-20076.

Smith, W. L., & Lands, W. E. M. (1972) *Biochemistry 11*, 3276−3285.

Smith, W. L., Eling, T. E., Kulmacz, R. J., Marnett, L. J., & Tsai, A.-L. (1992) *Biochemistry 31*, 3-7.

Tsai, A.-L., Palmer, G., & Kulmacz, R. J. (1992) *J. Biol. Chem. 267*, 17753−17759.

Tsai, A.-L., Hsi, L. C., Kulmacz, R. J., Palmer, G., & Smith, W. L. (1994) *J. Biol. Chem. 269*, 5085−5091.

Tsai, A.-L., Kulmacz, R. J., & Palmer, G. (1995) *J. Biol. Chem. 270*, 10503−10508.

van der Ouderaa, F. J., Buytenhek, M., Nugteren, D. H., & van Dorp, D. A. (1977) *Biochim. Biophys. Acta 487*, 315−331.

BI950069X